

Multiboson measurements in ATLAS and CMS

Antonio Giannini,^{a,*} on behalf of the ATLAS and CMS Collaborations

^a*Universita degli Studi di Napoli Federico II and INFN,
Complesso Universitario di Monte Sant'Angelo, Via Cinthia, 21, Napoli (Italy)*

E-mail: antonio.giannini@cern.ch

The multiboson final states allow to perform several measurements and to probe the Standard Model (SM) predictions with the amount of data collected at the LHC. Both the ATLAS and the CMS collaborations published new and interesting measurements in diboson and triboson final states selected in the Run 2 datasets corresponding to an integrated luminosity of about 139 fb^{-1} . Signatures with fully reconstructed systems (4-leptons), with missing energy (WZ and WW+jets) and photon associated final states ($W\gamma$ and $V\gamma\gamma$) have been exploited. Differential cross sections have been measured and the study of other properties such as the boson polarisation or the Radiation Amplitude Zero (RAZ) effect have been performed. Furthermore, constraints of the SM properties with precision higher and higher allow to perform Beyond Standard Model (BSM) physics results in the Effective Field Theory (EFT) framework.

*The Ninth Annual Conference on Large Hadron Collider Physics - LHCP2021
7-12 June 2021
Online*

*Speaker

1. Introduction

Multiboson production cross sections are among the most accessible physical observables at the energies of the LHC. Their relatively high values coupled with the high purity of multileptonic final states and their high sensitivity to variations in the SM trilinear gauge couplings (TGC) and quadrilinear gauge couplings (QGC) make them a powerful experimental tool to study the behaviour of the electroweak sector of the SM. Furthermore, multiboson production are usually background processes for other SM studies, like for the Higgs sector, and for BSM searches. Therefore, the constraint of the multiboson production is an interesting result useful to several physics programs of both the ATLAS [1] and the CMS [2] collaborations.

2. Diboson and Triboson processes

Several SM processes contribute to the production of diboson and triboson final states, with the possibility of additional contributions from BSM physics. The dominant SM contribution with 4 leptons in the final state is from the quark-induced t-channel $q\bar{q} \rightarrow 4l$ process, shown in Fig. 1 left. The associated production of a W and a Z boson is interesting because of the charged final state; it is completely dominated at tree level by qq' initial states, illustrated in Fig. 1 middle left. Two leading processes contribute to WW production: $q\bar{q} \rightarrow WW$ in the t- and s-channel (Fig. 1 middle right) and loop-induced gluon-gluon fusion processes $gg \rightarrow WW$. The photon in an associated $W\gamma$ production can be produced as either initial- or final-state radiation (Fig. 1 right), in addition to the contribution involving the TGC vertex. A photon pair can be produced associated to a W/Z boson via a QGC vertex.

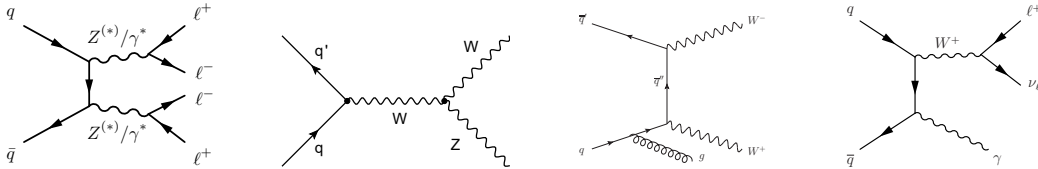


Figure 1: Feynman diagrams of few processes involved in the multiboson production at the pp collisions. 4 leptons quark-induced t-channel $q\bar{q} \rightarrow 4l$ (left), WZ s-channel $qq' \rightarrow WZ$ (middle left), WW+jets t-channel $q\bar{q} \rightarrow WW$ (middle right) and W plus initial state photon $q\bar{q} \rightarrow W\gamma$ (right) productions [3], [4], [5], [6].

The 4 leptons final state is fully reconstructed, while the W boson associated final states can not be fully reconstructed due the presence of missing energy (E_T^{miss}). Data are found to agree with the SM predictions for the invariant mass of the 4 leptons (Fig. 2 left) and for the transverse mass of the electron-muon system in a WW production (Fig. 2 right). Observed data are found consistent with SM predictions for photon associated final states, the W peak (left) and the transverse momentum (p_T) of a di-photon system (right) are shown in Fig. 3.

3. Cross section measurements

The ATLAS measurement of the 4 leptons production cross section at 13 TeV center of mass energy corresponds to 88.9 ± 3.0 (*total*) fb [3]. The measurement has been performed in different

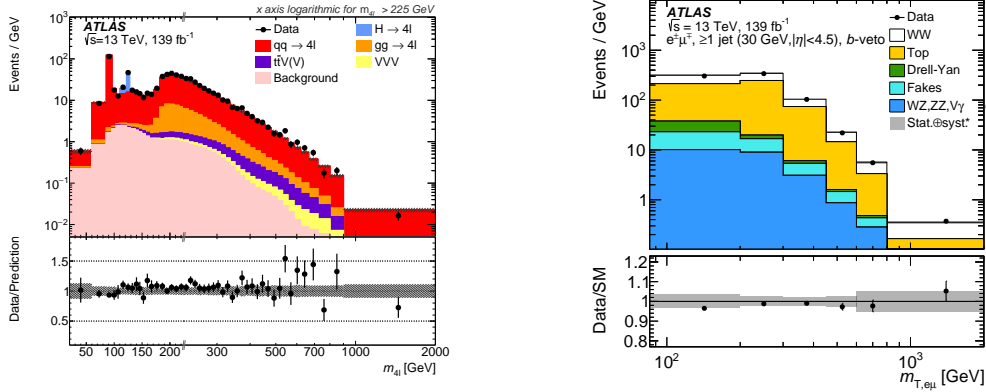


Figure 2: Observed reconstruction level m_{4l} distribution compared with the SM prediction, using Sherpa simulation (left). Signal region reconstruction level distribution of the $m_T^{e\mu}$ (right). For both plots, the shaded band in the ratio panel gives the total statistical and systematic uncertainty in the SM expectation [3], [5].

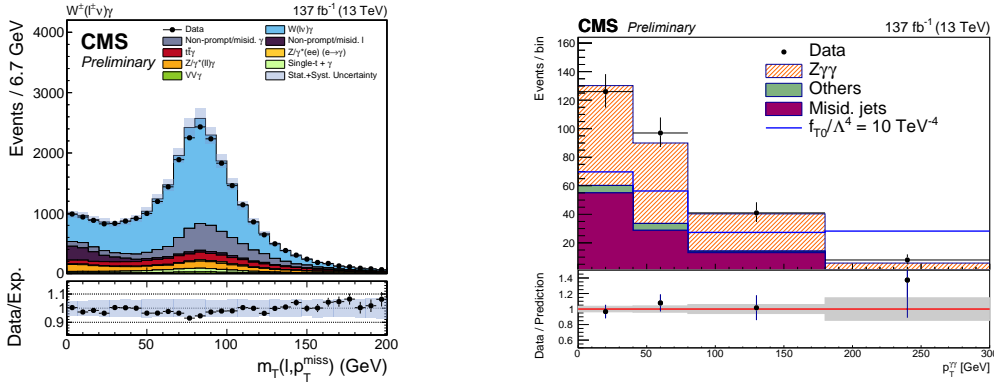


Figure 3: Distribution of the transverse mass $m_T(l, p_T^{\text{miss}})$ observable in the $W\gamma$ final state (left) and of the transverse momentum of the diphoton system for the $Z\gamma\gamma$ muon channel (right). For both plots, the shaded band in the ratio panel gives the total statistical and systematic uncertainty in the SM expectation [6], [7].

regions of the m_{4l} spectrum, targeting the $Z \rightarrow 4l$, $H \rightarrow 4l$, off- and on-shell ZZ contributions and as function of several kinematic variables [3]. The 13 TeV cross section for $WZ \rightarrow 3l\nu$ final state from the CMS collaboration is measured to be $50.6 \pm 1.9 \text{ pb}$ [4]. For the first time at the LHC, differential measurements of the WW production are performed in a jet-inclusive phase space by the ATLAS experiment [5]. The measured 13 TeV cross section is $258 \pm 4(\text{stat}) \pm 25(\text{syst}) \text{ fb}$; the combination of measurements with and without jets improves the precision up to 10% uncertainty. Differential cross-sections result in good agreement with SM expectations and they are shown for the p_T of the leading jet and the m_T of the electron-muon system in Fig. 4. The CMS collaboration measured the differential cross section at 13 TeV for $W\gamma$ associated production as function of several kinematic variables [6]. The result as a function of the photon p_T (Fig. 5 left) is in good agreement with the SM within the uncertainties, the systematic component dominates at low p_T (4 – 5%) while the statistical one (40%) in the highest bin. According to the RAZ effect [8], the interference between the Leading Order (LO) $W^{\pm}\gamma$ production diagrams result in a cross section that vanishes in specific phase space regions (Fig. 5 right), interesting for new physics effects. Finally, the first

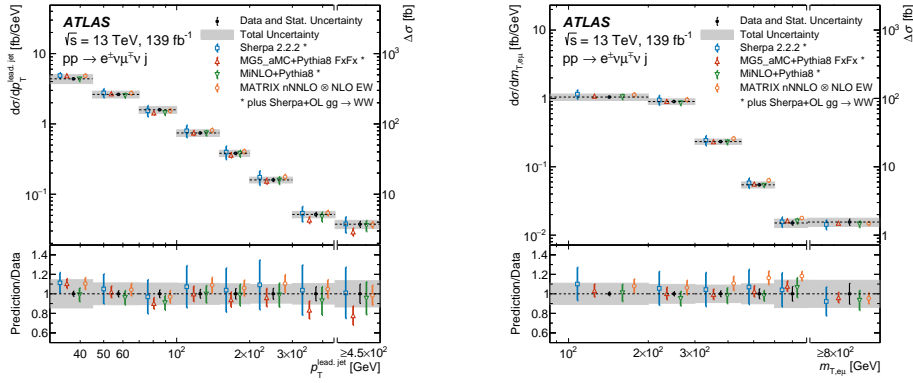


Figure 4: Measured fiducial cross-sections of WW+jets production for the leading jet p_T and transverse mass m_T of the $e - \mu$ system. The points show the measured cross-section values with error bars giving the statistical uncertainty and solid bands indicating the size of the total uncertainty. The results are compared with several MC generators [5].

measurement of a W or Z boson production in association with two photons associated production at 13 TeV, has been performed from the CMS experiment [7].

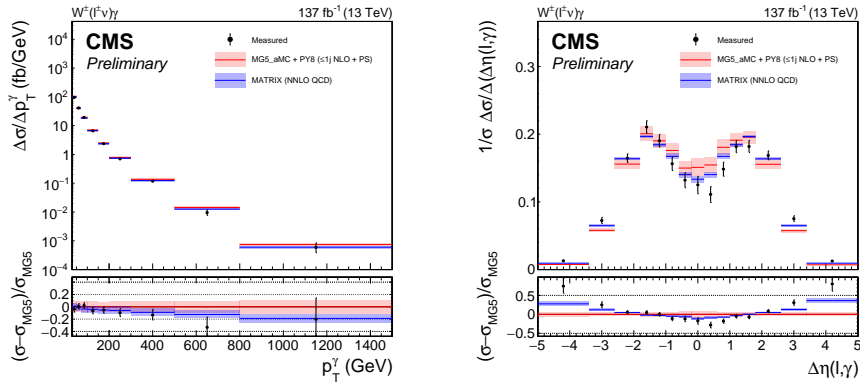


Figure 5: The measured p_T^γ differential cross sections (left), compared to the MG5_aMC+PY8 Next-to-LO (NLO) and MATRIX Next-to-NLO (NNLO) predictions; the shaded bands give the corresponding missing higher order uncertainties. The measured $\Delta\eta(l, \gamma)$ differential cross sections (right); the RAZ effect is expected in the region $\Delta\eta(l, \gamma) \sim 0$ [6].

4. Boson polarisation measurement

Non-resonant diboson production prefers to originate transverse polarized bosons. Fig. 6 left shows the polarization angle in the helicity frame (HF); good agreement with SM is found for the observed data [4]. One-dimensional confidence intervals for each polarization fraction and a two-dimensional confidence region are derived (Fig. 6 right). The presence of longitudinally polarized Z bosons is observed with a significance way above the conventional 5σ observation threshold, while longitudinally polarized W bosons are observed with an observed (expected) significance of 5.6σ (4.3σ). This represents the first observation of longitudinally polarized W bosons in the WZ channel.

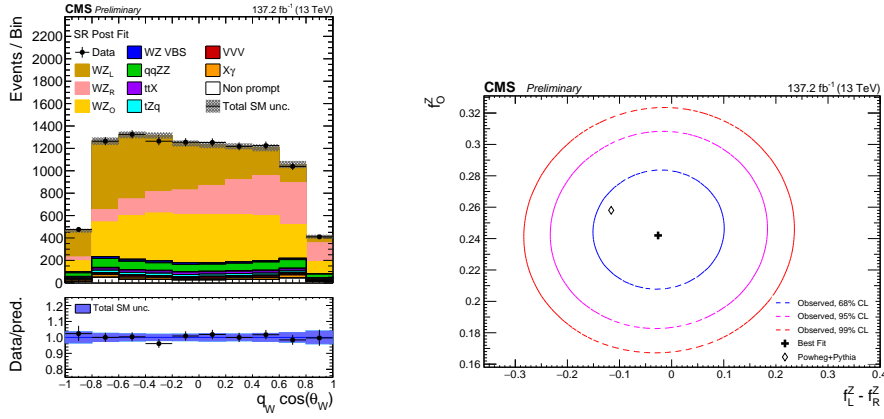


Figure 6: Distribution of the cosine of the polarization angle for the W boson in the inclusive charged final state (left). Confidence regions in the $f_{LR} - f_0$ parameter plane for the Z boson polarization (right) [4].

5. EFT interpretations

The measurement of anomalous self-interacting vector boson vertices from the theoretical predictions (aTGC or aQGC) could lead to indirect evidence of new physics. A parametrisation of predictions involving anomalous couplings, independent of a specific new physics model, can be performed in the EFT framework [9]; several and interesting results have been reached recently by the ATLAS and CMS collaborations analysing the 13 TeV data [3], [4], [5], [6], [7]. The dimension and the type of the operators as well as the main discriminants used are summarised in Table 1.

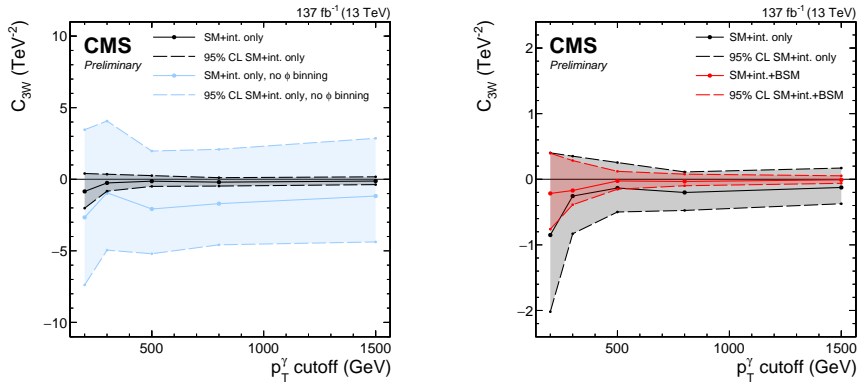


Figure 7: Best-fit values of C_{3W} and corresponding 95% CL confidence intervals as a function of the maximum p_T^γ bin included in the fit. Measurement without (left) and with (right) the binning in $|\phi_f|$ [6].

The interference term between the SM and the BSM is cancelled in the high energy regime of a diboson final state and this is due to the polarisation states predicted by the SM and the BSM physics. Usually, the interference resurrection can be reached requiring some extra activity or using the HF. The constraints on the C_{3W} coefficient are derived with and without the binning in the azimuthal angle ($|\phi_f|$) of the lepton in the HF in order to demonstrate the interference resurrection given by the improvement in sensitivity to the interference component up to a factor ten (Fig. 7).

Operators	4leptons [3]	WZ [4]	WW + jets [5]	W γ [6]	V $\gamma\gamma$ [7]
dimensions	dim-6	dim-6	dim-6	dim-6	dim-8
types	H/V/leptons	c_W, c_{3W}	c_W	c_{3W}	aQGC
discriminant	$m_{4l}, m_{34}, \Delta\phi_{ll}$	M_{WZ}	$M_{e\mu}$	$p_T^\gamma - \phi$	$p_T^{\gamma\gamma}$

Table 1: Dimensionality, types and discriminants involved in the main results published during the last year about the EFT constraints [3], [4], [5], [6], [7].

6. Summary

ATLAS and CMS collaborations have performed several multiboson measurements using the full LHC Run 2 datasets. The new results made public during the first part of the 2021 refer to fully-leptonic final states, E_T^{miss} , jets and photons associated boson productions. Cross section measurements have been improved or performed for the first time at the current 13 TeV energy finding an overall good agreement with the SM predictions both in inclusive and differential measurements. Polarised SM bosons have been observed and EFT constraints have been set for several operators.

References

- [1] ATLAS collaboration, *The ATLAS Experiment at the CERN Large Hadron Collider*, *JINST* **3** (2008) S08003.
- [2] CMS collaboration, *The CMS Experiment at the CERN LHC*, *JINST* **3** (2008) S08004.
- [3] ATLAS collaboration, *Measurements of differential cross-sections in four-lepton events in 13 TeV proton-proton collisions with the ATLAS detector*, *JHEP* **07** (2021) 005 [2103.01918].
- [4] CMS collaboration, *Measurement of the $pp \rightarrow WZ$ inclusive and differential cross sections, polarization angles and search for anomalous gauge couplings at $\sqrt{s} = 13$ TeV*, *CMS-PAS-SMP-20-014*.
- [5] ATLAS collaboration, *Measurements of $W^+W^- + \geq 1$ jet production cross-sections in pp collisions at $\sqrt{s} = 13$ TeV with the ATLAS detector*, *JHEP* **06** (2021) 003 [2103.10319].
- [6] CMS collaboration, *$W^\pm\gamma$ differential cross sections and effective field theory constraints at $\sqrt{s} = 13$ TeV*, *CMS-PAS-SMP-20-005*.
- [7] CMS collaboration, *Measurements of the $pp \rightarrow W^\pm\gamma\gamma$ and $pp \rightarrow Z\gamma\gamma$ cross sections at $\sqrt{s} = 13$ TeV and limits on anomalous quartic gauge couplings*, 2105.12780.
- [8] U. Baur, S. Errede and G. Landsberg, *Rapidity correlations in $W\gamma$ production at hadron colliders*, *Physical Review D* **50** (1994) 1917–1930.
- [9] C. Degrande, N. Greiner, W. Kilian, O. Mattelaer, H. Mebane, T. Stelzer et al., *Effective field theory: A modern approach to anomalous couplings*, *Annals of Physics* **335** (2013) 21–32.